Bioconjugate Chemistry

Article

pubs.acs.org/bc

Peptide-Based Vector of VEGF Plasmid for Efficient Gene Delivery *in Vitro* and Vessel Formation *in Vivo*

Wei Qu,[†] Si-Yong Qin,[†] Shan Ren,[‡] Xue-Jun Jiang,[‡] Ren-Xi Zhuo,[†] and Xian-Zheng Zhang*,[†]

[†]Key Laboratory of Biomedical Polymers of Ministry of Education & Department of Chemistry, Wuhan University, Wuhan 430072, P. R. China

[‡]Department of Cardiology, Renmin Hospital of Wuhan University, Wuhan 430060, P. R. China

Supporting Information

ABSTRACT: Critical limb ischemia is regarded as a potentially lethal disease, and the treatment effects of existing therapies are limited. Here, in order to develop a potential approach to improve the therapy effects, we designed a peptide of TAT-PKKKRKV as the vector for $VEGF_{165}$ plasmid to facilitate *in vivo* angiogenesis. In *in vitro* studies, TAT-PKKKRKV with low cytotoxicity exhibited efficient transfection ability either with or without serum. Additionally, application of TAT-PKKKRKV/$VEGF_{165}$ complexes in hindlimb ischemia rats obviously promoted the expression of VEGF protein, which further enhanced effective angiogenesis. The results indicated that TAT-PKKKRKV is an efficient gene vector with low toxicity both *in vitro* and *in vivo*, which has great potential for clinical gene therapy.

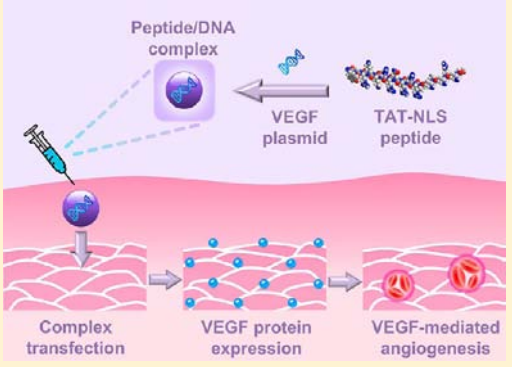

INTRODUCTION

Compared with traditional chemotherapy, gene therapy is much smarter and more accurate and effective, which can be attributed to its unique remedy ability based on genic levels.[1−3] Since the first human clinical gene therapy trial, thousands of clinical trials have been conducted throughout the world.[4−6] As the primary issue for successful gene therapy, gene vectors keep naked nucleic acids from degradation and make subsequent delivery more efficient. Existing gene vectors are generally divided into viral vectors and nonviral vectors. Viral gene vectors, as the initial natural vehicle for gene delivery, have been well studied.[7] Although viral vectors have exhibited high transfection efficiency, their inborn immunogenicity, toxicity, and scale-up procedure limitations have restricted further applications in clinical therapy.[5] In addition, current gene therapy research mainly focuses on nonviral gene vectors for their ease of preparation and relatively low cytotoxicity.[8−10]

Among their counterparts, cationic peptides composed of natural amino acids are newly developed nonviral gene vectors with good biocompatibility and inherent biodegradability. TAT peptide (Tyr-Gly-Arg-Lys-Lys-Arg-Arg-Gln-Arg-Arg-Arg, YGRKKRRQRRR) is one of the most frequently utilized cell-penetrating peptides (CPPs), with amino acid sequences readily crossing the cell membrane.[11−13] Derived from the trans-activating transcriptional activators of human immunodeficiency virus type 1 (HIV-1 TAT protein), the arginine-rich region of TAT peptide facilitates cellular internalization.[14,15] TAT peptide has been proven to be potent for promoting transfection efficiency by overcoming the first barrier of gene delivery.[16−18] Furthermore, it was found that the delivered gene was expressed in less than 1% of cells when injection occurred in cytoplasm, while the ratio rose up to 50% when injection directly occurred in nucleus.[19] Therefore, efficient nuclear accumulation of delivered gene is considered a critical step in gene therapy. A peptide sequence of nuclear localization signal (NLS) with nuclear import improvement ability has been identified from the large T antigen of the SV40 virus,[20] and a typical example of NLS is the 7-amino acid sequence (Pro-Lys-Lys-Lys-Arg-Lys-Val, PKKKRKV), which has been reported to enhance gene delivery successfully.[21,22]

Critical limb ischemia is regarded as a potentially lethal disease. In many practical cases, surgical or catheter-based revascularization procedures are not possible, and it leads to over 150 000 amputations each year in the United States.[23] The present treatments chiefly involve molecular and cell-based therapies to improve angiogenesis and collateral artery enlargement.[24] However, the outcomes of cell-based therapies in hindlimb ischemia animals have not been satisfactory.[25−28] By utilizing the most specific and powerful angiogenic factor, vascular endothelial growth factor (VEGF), clinical ischemic heart and peripheral artery disease trials have already been investigated with naked DNA or adenoviral vectors, which exhibiting positive therapy effects.[29,30]

In this study, to utilize nonviral vectors with good biocompatibility for stimulating angiogenesis in hindlimb ischemia model, a peptide with integrated sequence of TAT-PKKKRKV as the carrier for VEGF plasmid was synthesized. The *in vitro* cytotoxicity and transfection efficiencies of TAT-

Received: December 20, 2012
Revised: March 26, 2013
Published: May 10, 2013

   dx.doi.org/10.1021/bc300677n | *Bioconjugate Chem.* 2013, 24, 960−967

PKKKRKV were evaluated. Moreover, its *in vivo* toxicity and angiogenesis effects were also examined.

EXPERIMENTAL PROCEDURES

Materials. Thioanisole was purchased from Acros and used as supplied. *N*-Fluorenyl-9-methoxycarbonyl (Fmoc) protected L-amino acids (Fmoc-Tyr(tBu)-OH, Fmoc-Gly-OH, Fmoc-Arg(Pbf)-OH, Fmoc-Lys(Boc)-OH, Fmoc-Gln(Trt)-OH, Fmoc-Pro-OH, and Fmoc-Val-OH), 2-chlorotrityl chloride resin (100−200 mesh, loading: 1.32 mmol/g), *o*-benzotriazole-*N*,*N*,*N*′,*N*′-tetramethyluroniumhexafluorophosphate (HBTU) and *N*-hydroxybenzotriazole (HOBt) were purchased from GL Biochem Ltd. (Shanghai, China) and used without further purification. *N*,*N*′-Dimethylformamide (DMF), dimethyl sulfoxide (DMSO), dichloromethane (DCM), and diisopropylethylamine (DiEA) were obtained from Shanghai Reagent Chemical Co. (China), and distilled prior to use. Phenol, piperidine, trifluoroacetic acid (TFA), and 1,2-ethanedithiol (EDT) were provided by Shanghai Reagent Chemical Co. (China), and used directly.

QIAfilter plasmid purification Giga Kit (5) was purchased from Qiagen (Hilden, Germany). GelRed was provided by Biotium (CA, USA). Dulbecco's Modified Eagle's Medium (DMEM), Dulbecco's phosphate buffered saline (PBS), 3-[4,5-dimethylthiazol-2-yl]-2,5-diphenyltetra-zoliumbromide (MTT), fetal bovine serum (FBS), penicillin−streptomycin, and trypsin were purchased from Invitrogen Corp. The Micro BCA protein assay kit was purchased from Pierce. All other reagents were of analytical grade and used as received.

Cell Culture and Amplification of Plasmid DNA. African green monkey kidney fibroblast cells (COS-7), human embryonic kidney transformed 293 cells (293T), and human cervix carcinoma cells (HeLa) were incubated in DMEM medium with 10% FBS and 1% antibiotics (penicillin−streptomycin, 10 000 U/mL) at 37 °C in a humidified atmosphere containing 5% CO_2.

pGL-3 plasmid used as luciferase reporter gene was transformed in *Escherichia coli* JM109, and green fluorescent protein-tagged $VEGF_{165}$ expression plasmid (pEGFP-N1-$VEGF_{165}$) was transformed in *Escherichia coli* DH5α. Both plasmids were amplified in LB medium at 37 °C overnight, and purified by an EndoFree QiAfilter Plasmid Giga Kit (5). Then the purified plasmids were dissolved in deionized water and stored at −20 °C. The concentration and purity of plasmids were measured by ultraviolet (UV) absorbance at 280 and 260 nm.

Synthesis of Peptide and Preparation of TAT-PKKKRKV/DNA Complexes. TAT-PKKKRKV was prepared manually by employing solid phase peptide synthesis technique based on classical strategy of Fmoc chemistry.[31] Briefly, the loading of the first peptide residue to 2-chlorotrityl chloride resin was carried out in a DMF solution with 2 equiv (relative to the substitution degree of resin) Fmoc-protected amino acid and 4 equiv of DiEA for 2 h at room temperature. After deprotection of Fmoc groups with 20% piperidine/DMF (v/v), the rest of the peptide residues were coupled in turn by reacting with 2 equiv of Fmoc-protected amino acid, and 4 equiv of HBTU, HOBt, and DiEA, respectively, for 3 h. After the peptide was synthesized, the resin was washed with DMF and DCM, and dried under vacuum overnight. To deprotect peptide side chains and detach the expected peptides from the solid support, the dried resin was stirred with a mixture containing TFA (83%), phenol (6.3%), thioanisole (4.3%), H_2O (4.3%), and EDT (2.1%) for 2 h at room temperature. The supernatant was collected after filtration and further concentrated to a viscous solution by rotary evaporation. The crude product was obtained by precipitating in cold ether. After vacuum-drying overnight, the precipitate was dissolved in distilled water and freeze-dried. The molecular weight of the peptide was confirmed by electrospray ionization mass spectrometry (ESI-MS) and time-of-flight mass spectrometry (TOF-MS).

The TAT-PKKKRKV/DNA complexes of varying weight ratios were prepared by mixing a particular volume of TAT-PKKKRKV solution with 5 μL DNA solution (200 ng/μL). The system was incubated for 30 min at 37 °C to form stable TAT-PKKKRKV/DNA complexes.

Agarose Gel Retardation Assay. The TAT-PKKKRKV/DNA complexes were prepared with varying weight ratios ranging from 0 to 30 by adding appropriate volumes of TAT-PKKKRKV solution to pGL-3 plasmid (0.5 μL, 200 ng/μL in water). The complexes were diluted to a total volume of 8 μL with NaCl solution (150 mM), and then the complexes were incubated at 37 °C for 30 min. After that, the complexes were electrophoresed in the 0.7% (w/v) agarose gel containing GelRed and with Tris-acetate (TAE) running buffer at 80 V for 40 min. DNA was visualized with a UV lamp by the Vilber Lourmat imaging system (France).

Particle Size and Zeta Potential Measurement. The particle size and zeta potential were measured by Nano-ZS ZEN3600 (MALVERN Instruments) at 25 °C. The TAT-PKKKRKV/DNA complexes were prepared with varying weight ratios ranging from 1 to 30 by adding appropriate volumes of peptide solution to pGL-3 plasmid (5 μL, 200 ng/μL in water). After incubation at 37 °C for 30 min, the complexes were diluted to 1 mL with distilled water or NaCl solution (150 mM) for zeta potential and size measurement respectively.

***In Vitro* Cytotoxicity Assay.** The cytotoxicity of TAT-PKKKRKV was evaluated with COS-7, 293T, and HeLa cells by MTT assay. Briefly, cells were seeded respectively in 96-well plates at a density of 6000 cells/well and cultured in DMEM (200 μL) containing 10% FBS for 24 h. Then TAT-PKKKRKV solution of different concentrations was added to the wells. The culture medium was replaced with fresh medium (200 μL) after 48 h, and MTT solution (20 μL, 5 mg/mL) was added to each well and incubated for 4 h. After that, the medium was removed and DMSO (200 μL) was added. The optical density (OD) was measured at 570 nm using a microplate reader (Bio-Rad, Model 550, USA). The relative cell viability was calculated as: cell viability (%) = ($OD570_{(sample)}$/$OD570_{(control)}$) × 100, where $OD570_{(control)}$ was obtained in the absence of TAT-PKKKRKV and $OD570_{(sample)}$ was obtained in the presence of TAT-PKKKRKV.

***In Vitro* Transfection.** The transfection efficiency of TAT-PKKKRKV/DNA complexes was evaluated with pGL-3 plasmid. COS-7, 293T, and HeLa cells were seeded in 24-well plates at a density of 6×10^4 cells/well and cultured with 1 mL DMEM containing 10% FBS for 24 h respectively. The complexes of different weight ratios were prepared by mixing 1 μg plasmid DNA and corresponding volumes of TAT-PKKKRKV solution at 37 °C for 30 min. Then the complexes were added into plates with 1 mL DMEM (serum-free or containing 10% FBS) and incubated for 4 h at 37 °C. Thereafter, the medium was replaced with fresh DMEM containing 10% FBS and the cells were cultured for another 44

dx.doi.org/10.1021/bc300677n | *Bioconjugate Chem.* 2013, 24, 960−967

h. For luciferase assay, cells were washed by PBS after removing the medium. Then the cells in each well were lysed using 200 μL reporter lysis buffer (Pierce). The relative light units (RLUs) were measured with chemiluminometer (Lumat LB9507, EG&G Berthold, Germany). The total protein was measured according to a BCA protein assay kit (Pierce) and luciferase activity was expressed as RLU/mg protein.

For detecting pEGFP-N1-$VEGF_{165}$ plasmid expression, transfected cells with green fluorescent proteins were directly observed under inverted microscope (IX 70, Olympus, Japan). The micrographs were obtained at the magnification of 100× and recorded using CoolSNAP-Pro (4.5.1.1).

Generation of Hindlimb Ischemia Animal Model and Experimental Protocols. To study the effects induced by TAT-PKKKRKV/$VEGF_{165}$ complexes, hindlimb ischemia model was adopted, by use of 8−12 weeks Wistar rats (Wuhan University Center for Animal Experiment, China). Briefly, the rats underwent unilateral ligation and excision of the right femoral artery and its branches, under anesthesia with an intraperitoneal injection of pentobarbital sodium (50 mg/kg). For the complex group, 0.3 mL TAT-PKKKRKV/DNA complex solution containing $VEGF_{165}$ plasmid (0.1 mg) was injected intramuscularly. For $VEGF_{165}$ plasmid group, 0.3 mL solution containing 0.1 mg $VEGF_{165}$ plasmid was directly administered by intramuscular injection, and left hindlimb injection with an equal amount of PBS was used as the control group. Two weeks later, the thigh muscles were harvested and fixed with 4% paraformaldehyde solution for further histological analysis. All protocols were performed in compliance with the National Guideline on the Care and Use of Laboratory Animals.

***In Vivo* Cytotoxity and Angiogenic Effects.** For each tissue sample, 5-μm-thick paraffin-embedded sections were stained with hematoxylin and eosin to assess cytotoxity induced by TAT-PKKKRKV/$VEGF_{165}$ complexes directly.

In addition, the expression of VEGF protein and angiogenic effects improved by TAT-PKKKRKV/$VEGF_{165}$ complexes were determined in histological sections by immunohistochemistry, with staining of VEGF, α-SMA, CD31, and Factor VIII, respectively. For staining, tissue sections were rehydrated, and incubated with methanol containing 0.3% hydrogen peroxide for 20 min to block endogenous peroxidase activity. Then, sections were incubated overnight with primary antibody (Santa Cruz, dilution 1:200) at 4 °C, followed by an HRP-conjugated secondary antibody (DAKO, dilution 1:300) for 1 h at 4 °C. Stainings were visualized with diaminobenzidine by an inverted microscope (Olympus IX 70, Japan). The micrographs were recorded using CoolSNAP-Pro (4.5.1.1).

RESULTS AND DISCUSSION

Synthesis and Characterization of TAT-PKKKRKV. As typical peptides of CPP and NLS, TAT peptide and PKKKRKV have been proven to facilitate cellular internalization and nuclear import, respectively.[32] Here, to utilize the advantages of both peptides for efficient gene delivery, TAT peptide and PKKKRKV were designed to synthesize into an integrated sequence as TAT-PKKKRKV, as illustrated in Figure 1. TAT-PKKKRKV was synthesized manually employing a classical strategy of Fmoc chemistry.[31] The molecular weight was analyzed by using ESI-MS (LCQ Advantage, Finigan, USA). ESI-MS *m*/*z*: $[M+3H]^{3+}$ calculated for TAT-PKKKRKV, 809.3; found, 809.4. Moreover, TOF-MS was used to confirm the peptide structure. The result is provided in Supporting Information (Figure S1).

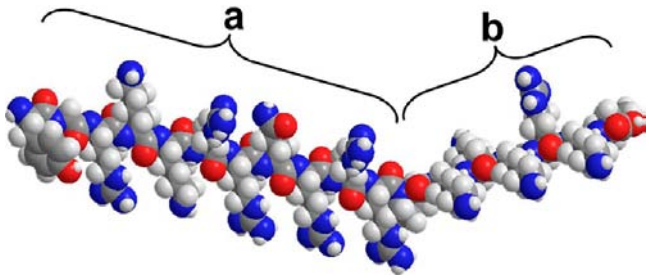

Figure 1. Structure of TAT-PKKKRKV fabricated from natural amino acids. Schematic of TAT-PKKKRKV with (a) TAT, for enhancement of intracellular transduction, (b) PKKKRKV, for promotion of nuclear uptake. Atoms of TAT-PKKKRKV were represented with different color as white: H; gray: C; blue: N; and red: O.

Peptide-DNA Complexation and Characterization. As a peptide with high content of basic amino acids, TAT-PKKKRKV is positively charged in physiological conditions, which is just opposite to DNA. Therefore, TAT-PKKKRKV/DNA complexes were prepared by electrostatic interaction between cationic peptide and negative DNA after incubation. Generally, DNA binding ability is regarded as a prerequisite for gene vector.[33] To evaluate the association between TAT-PKKKRKV and DNA with various w/w ratios ranging from 0 to 30, TAT-PKKKRKV/DNA complexes were electrophoresed by gel retardation assay. As shown in Figure 2, TAT-PKKKRKV was able to compactly condense DNA above the w/w ratio of 5, which indicated the tight association between TAT-PKKKRKV and DNA for further transfection study.

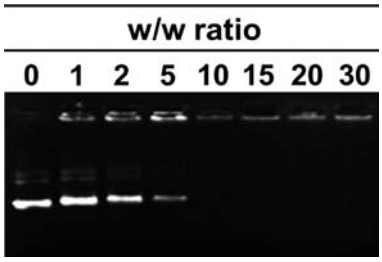

Figure 2. Agarose gel electrophoresis retardation assay of TAT-PKKKRKV/DNA complexes at w/w ratios ranging from 0 to 30.

The DNA condensing ability of vectors can be also revealed by the particle size and vector/DNA complexes with appropriate size promises effective cellular uptake for gene translocation.[34] The particle size of TAT-PKKKRKV/DNA complexes at w/w ratios ranging from 1 to 30 were measured in 150 mM NaCl solution to simulate physiological ionic strength condition. As presented in Figure 3A, with increasing weight ratios, the particle size of TAT-PKKKRKV/DNA complexes decreased sharply before reaching the ratio of 5. When the ratio was relatively low, the combination between TAT-PKKKRKV and DNA mainly occurred at molecular level mediated by electrostatic interaction. With increasing content of positive vector molecules, TAT-PKKKRKV could combine and condense negative DNA more effectively, which might cause the complexation status from loose to tight between TAT-PKKKRKV and DNA. At w/w ratios higher than 5, the particle size increased slightly with a top value not exceeding 200 nm. After the ratio reached 5, the association between TAT-

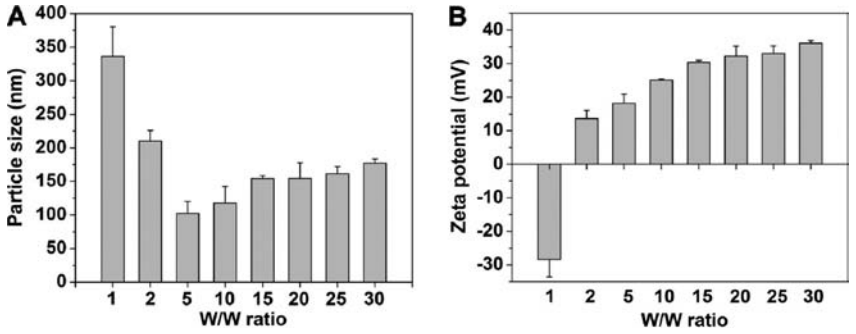

Figure 3. (A) Particle size and (B) zeta potential of TAT-PKKKRKV/DNA complexes at w/w ratios ranging from 1 to 30. Data were shown as mean ± SD (n = 3).

PKKKRKV and DNA molecules was inclined to saturation. However, there still might be unpacked DNA molecules exposed to the surface of TAT-PKKKRKV/DNA complexes, which could induce mild aggregation among positive TAT-PKKKRKV/DNA complexes.

In nonspecific gene delivery, cellular uptake mainly depends on the interaction between negatively charged cell membranes and positively charged complexes. Relatively high surface charges are usually preferred for complex and cell interaction, and subsequent uptake and endocytosis.[9,35,36] As presented in Figure 3B, the zeta potential of TAT-PKKKRKV/DNA complexes increased with the growth of ratios ranging from 1 to 30. At weight ratios higher than 1, TAT-PKKKRKV/DNA complexes were positively charged with the maximum potential reaching 36 mV at the w/w ratio of 30. The upward trend was caused by the increasing content of cationic TAT-PKKKRKV, which might improve the endocytosis mediated by electrostatic interaction.

***In Vitro* Cytotoxicity.** The good biocompatibility of vectors is important for gene therapy in clinical trials. The cytotoxicity of TAT-PKKKRKV was evaluated by MTT assay. According to Figure 4, TAT-PKKKRKV exhibited no significant toxicity in

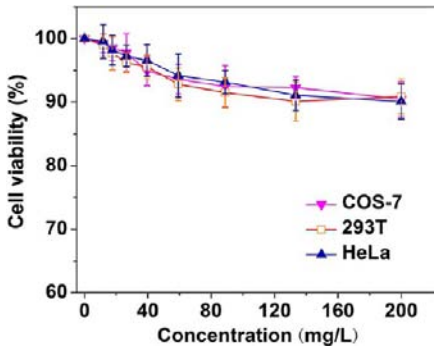

Figure 4. Cytotoxicity of TAT-PKKKRKV in COS-7, 293T, and HeLa cells. Data were shown as mean ± SD (n = 3).

COS-7, 293T, and HeLa cells. The relative cell viabilities of investigated concentrations were all higher than 90%, which was ascribed to the good biocompatibility of peptides consisted of natural amino acids. In subsequent *in vitro* transfection assays, the highest application concentration was 30 mg/L. The relatively high cell viability suggested that TAT-PKKKRKV would be safe for further research of gene therapy.

***In Vitro* Transfection.** The transfection efficiency of luciferase mediated by TAT-PKKKRKV/DNA complexes was tested in COS-7, 293T, and HeLa cells with weight ratios ranging from 1 to 30. The transfection assays were performed in conditions with 10% serum or without serum, respectively. As illustrated in Figure 5, the luciferase expression level was mainly influenced by the weight ratio of TAT-PKKKRKV/DNA complexes. In the cell lines studied above, the transfection efficiencies of TAT-PKKKRKV/DNA complexes exhibited similar trends. Before reaching peak values at the ratio of 10, the transfection efficiencies of complexes increased with increasing ratio. At the ratio higher than 10, the transfection efficiencies decreased with the ratio growth. Among different cell lines, TAT-PKKKRKV/DNA complexes presented higher transfection efficiency in 293T cells, with the peak values of 8.99×10^7 and 1.02×10^8 RLU/mg protein in the presence or absence of serum, respectively. Moreover, in order to investigate the effect of serum, the transfection was carried out in normal cell culture conditions with 10% serum and the results presented no significant differences in the above cell lines. For example, the transfection efficiency in COS-7 cells at ratio of 15 was 2.41×10^7 RLU/mg protein with serum and 2.53×10^7 RLU/mg protein without serum, respectively. As the basic demand for systemic delivery in *in vivo* application, a relatively high transfection efficiency of gene vectors in serum is necessary. In comparison with the transfection results without serum, the influence on transfection ability of TAT-PKKKRKV/DNA complexes was not obvious in the existence of serum. The comparable efficiencies indicated that TAT-PKKKRKV/DNA complexes were relatively stable in the presence of serum, which might benefit the further clinical applications.

In addition, according to the above results, TAT-PKKKRKV/$VEGF_{165}$ complex with an optimal weight ratio of 10 was adopted to study the *in vitro* transfection mediated by TAT-PKKKRKV. The green fluorescent protein expressions of pEGFP-N1-$VEGF_{165}$ plasmid in COS-7, 293T, and HeLa cells were shown in Figure 6. In different cell lines, distinct green fluorescence was observed. The density and luminance of fluorescence were similar in COS-7, 293T, and HeLa cells. Between the groups with or without serum, the status of green fluorescence exhibited no obvious differences. The results were consistent with the finding of luciferase transfection assay and further confirmed the transfection capability of TAT-PKKKRKV/$VEGF_{165}$ complexes *in vitro*.

In vivo angiogenesis assays by utilizing TAT-PKKKRKV peptide as the vector of $VEGF_{165}$ plasmid were further performed. As one of the most important angiogenic growth factors (GFs), VEGF involves in the neovascularization signaling pathways, which represent major driving forces for new blood vessel formation. Local gene delivery of VEGF

dx.doi.org/10.1021/bc300677n | *Bioconjugate Chem.* 2013, 24, 960−967

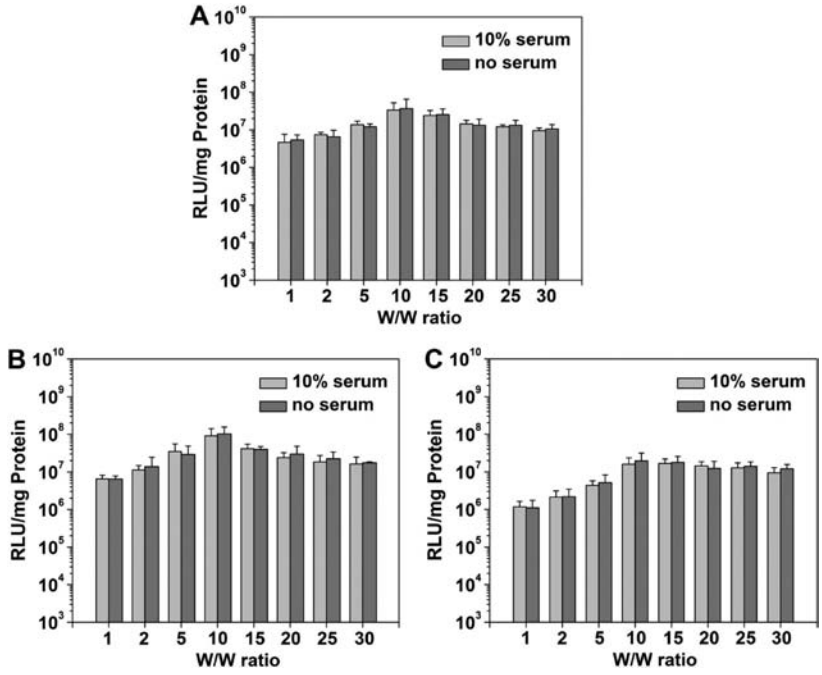

Figure 5. *In vitro* transfection efficiency of TAT-PKKKRKV/DNA complexes at w/w ratios ranging from 1 to 30 in (A) COS-7, (B) 293T, and (C) HeLa cells with 10% serum or with no serum, respectively. Data were shown as mean ± SD (n = 3).

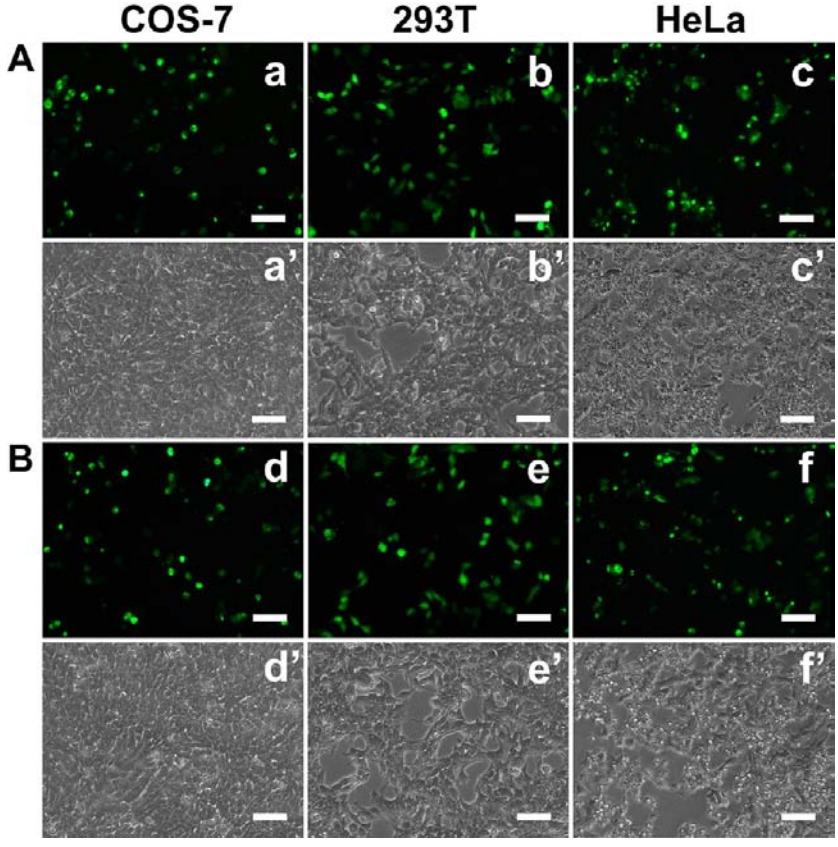

Figure 6. VEGF protein expression in COS-7, 293T, and HeLa cells transfected by TAT-PKKKRKV/VEGF$_{165}$ complexes (w/w = 10) (A) with 10% serum or (B) without serum. The green fluorescence images in COS-7, 293T, and HeLa cells were (a, b, c) and (d, e, f), respectively. The corresponding light inverted images were (a′, b′, c′) and (d′, e′, f′), respectively. Scale bars represent 100 μm.

plasmid is highly preferred for therapeutic angiogenesis.[37,38] The cells transfected by TAT-PKKKRKV/VEGF$_{165}$ complexes can subsequently express VEGF protein, which induces angiogenesis in succession.

dx.doi.org/10.1021/bc300677n | *Bioconjugate Chem.* 2013, 24, 960−967

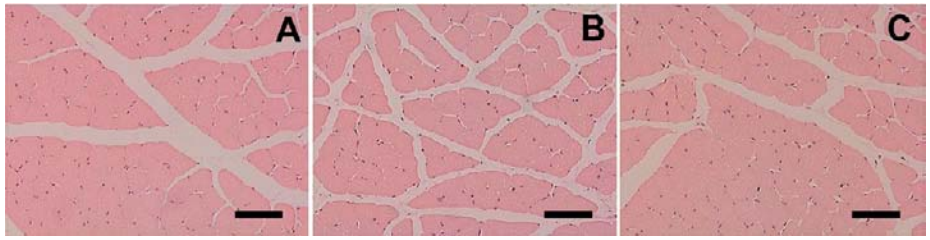

Figure 7. Histopathological examination of ischemic hindlimbs with hematoxylin-eosin staining of (A) TAT-PKKKRKV/$VEGF_{165}$ complexes group and (B) $VEGF_{165}$ plasmid group, while (C) PBS group was used as the control. Scale bars represent 100 μm.

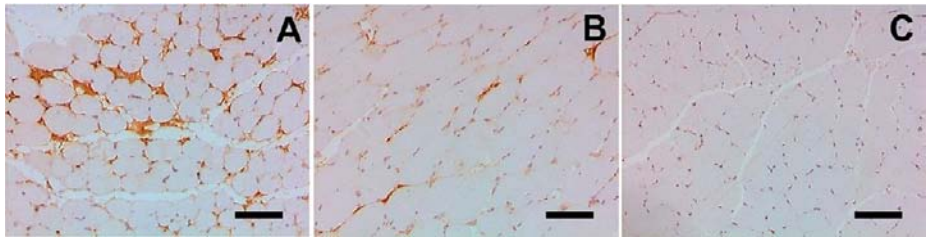

Figure 8. Immunohistochemical identification of VEGF protein expressed in ischemic hindlimbs of (A) TAT-PKKKRKV/$VEGF_{165}$ complexes group and (B) $VEGF_{165}$ plasmid group, while (C) PBS group acted as the control. Scale bars represent 100 μm.

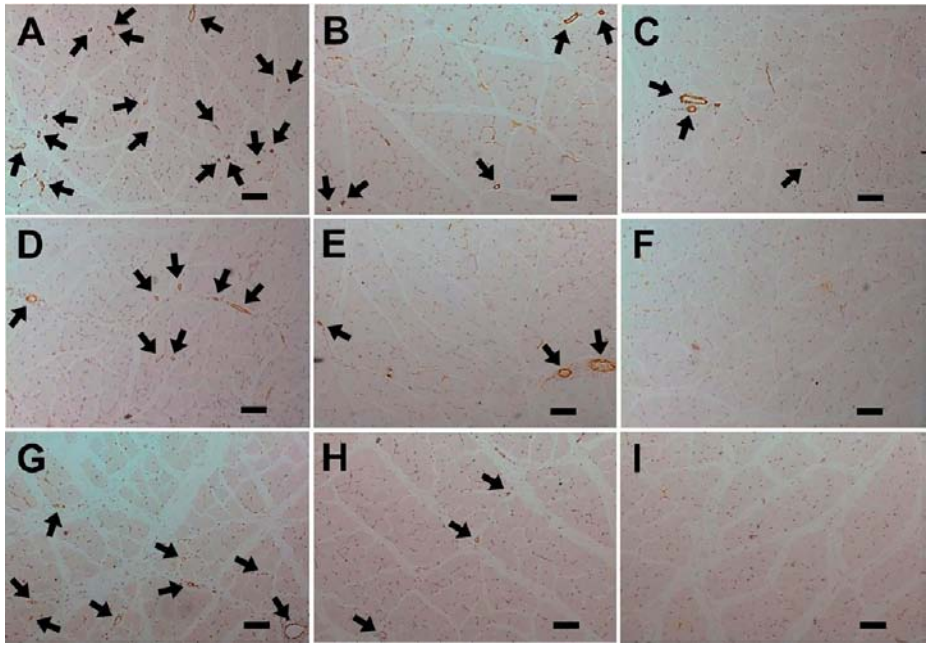

Figure 9. Representative microscopic photos of the vessels stained by α-SMA (A, B, C), CD31 (D, E, F), and Factor VIII (G, H, I) in ischemic hindlimbs. Among them, (A, D, G) belonged to TAT-PKKKRKV/$VEGF_{165}$ complexes group, (B, E, H) belonged to $VEGF_{165}$ plasmid group, and (C, F, I) of PBS group were used as the control. Arrows indicated the stained vessels. Scale bars represent 100 μm.

***In Vivo* Cytotoxicity.** The *in vivo* toxic level of gene vectors is usually considered to be the same important as the effect of gene therapy. The toxicity of TAT-PKKKRKV/$VEGF_{165}$ complexes in muscle cells of harvested tissue samples was assessed by histopathological examination. The microscopic photos of hematoxylin-eosin staining sections were presented in Figure 7. Among Figure 7A,B, and C, the muscle cells were morphologically normal with no signs of injury. Compared with PBS group, the structure of cytoplasm and nuclei in complexes group and $VEGF_{165}$ plasmid group was clear and intact. The cells were arrayed regularly with clear structure, which indicated that the treatment of either TAT-PKKKRKV/$VEGF_{165}$ complexes or $VEGF_{165}$ plasmid had no apparent cytotoxity to muscle cells.

***In Vivo* Angiogenic Effects.** To evaluate the *in vivo* angiogenesis effects of TAT-PKKKRKV/$VEGF_{165}$ complexes, the hindlimb ischemia model was adopted. The successful expression of proteins encoded by the delivered gene is an important objective of gene therapy. To observe the expression of VEGF protein in hindlimb ischemia rats, the obtained histological sections were analyzed by immunohistochemistry. As illustrated in Figure 8, a distinct overexpression of VEGF protein was observed in the complexes group, while the protein expression was limited in $VEGF_{165}$ plasmid group. Additionally, in PBS group, no obvious expression was discovered. The

dx.doi.org/10.1021/bc300677n | *Bioconjugate Chem.* 2013, 24, 960−967

obtained results demonstrated that TAT-PKKKRKV/$VEGF_{165}$ complexes could obviously enhance the expression of VEGF protein, which might further improve the generation of neovasculature.

Moreover, as the crucial step for ameliorating blood circulation in ischemic tissues, angiogenesis was considered to be a direct and effective approach.[39,40] For detecting the vessels in histological sections, immunohistochemical analysis was carried out with α-SMA, CD31, and Factor VIII staining, respectively (Figure 9). As pointed out by arrows in Figure 9A,B,C, α-SMA positive cells were stained strongly and consistently to indicate the vessels. Apparently, among the investigated groups, the vessels mostly appeared in the complexes group, whereas vessels in PBS group were the least. However, as SMA-positive components existed in both myoepithelial cells and vascular wall cells, the judgment accuracy of the vessels might be influenced.[41] Hence, to further identify vessels more specifically, CD31 and Factor VIII staining were performed.

As a transmembrane glycoprotein, CD31 is highly expressed in endothelium.[42] Factor VIII is localized selectively in Weibel-Palade bodies, which represent a unique type of endothelial cell-specific inclusion.[43] Both CD31 and Factor VIII are widely used endothelial markers for studying neovascular endothelium of angiogenesis.[44−46] As indicated in Figure 9D to I, the vessel number was highest in the complexes group, while the number decreased in $VEGF_{165}$ plasmid group, and in the PBS group, no vessel was identified. Overall, these results demonstrated that $VEGF_{165}$ protein was an effective angiogenic factor in ischemic tissue. Furthermore, the angiogenic ability was significantly enhanced by the use of vector of TAT-PKKKRKV. The hindlimb ischemia model represents quite a number of clinical situations for the patients with peripheral artery disease, which are candidates for angiogenesis therapy.[30] Therefore, the positive angiogenic effects of TAT-PKKKRKV/$VEGF_{165}$ complexes suggested that TAT-PKKKRKV is a promising vector for clinical gene therapy of limb ischemia.

CONCLUSIONS

In summary, this study developed an integrated peptide sequence of TAT-PKKKRKV as a promising vector for gene therapy. According to the results of *in vitro* investigations, TAT-PKKKRKV was exhibited to be an efficient gene vector with low cytotoxicity. Furthermore, the *in vivo* research indicated that the low toxicity TAT-PKKKRKV/$VEGF_{165}$ complexes could significantly promote the expression of VEGF protein, which further improved effective local angiogenesis. We believe TAT-PKKKRKV will be highly desirable for gene therapy of limb ischemia.

ASSOCIATED CONTENT

Supporting Information

The TOF-MS spectrum of TAT-PKKKRKV. This material is available free of charge via the Internet at http://pubs.acs.org.

AUTHOR INFORMATION

Corresponding Author

*Tel. and Fax: + 86 27 6875 4059. E-mail address: xz-zhang@whu.edu.cn (X. Z. Zhang).

Notes

The authors declare no competing financial interest.

ACKNOWLEDGMENTS

We acknowledge the financial support from the National Natural Science Foundation of China (51125014, 51233003) and the Ministry of Science and Technology of China (2011CB606202).

REFERENCES

(1) Leonard, W., and Thrasher, A. J. (2012) Gene therapy matures in the clinic Seymour. *Nat. Biotechnol. 30*, 588−593.
(2) Tomanin, R., Zanetti, A., Zaccariotto, E., D'Avanzo, F., Bellettato, C. M., and Scarpa, M. (2012) Gene therapy approaches for lysosomal storage disorders, a good model for the treatment of mendelian diseases. *Acta. Paediatr. 101*, 692−701.
(3) Li, G. P., Ye, L., Pan, J. S., Long, M. Y., Zhao, Z. Z., Yang, H. Y., Tian, J., Wen, Y. L., Dong, S. L., Guan, J., and Luo, B. M. (2012) Antitumoural hydroxyapatite nanoparticles-mediated hepatoma-targeted trans-arterial embolization gene therapy: in vitro and in vivo studies. *Liver Int. 32*, 998−1007.
(4) Edelstein, M. L., Abedi, M. R., and Wixon, J. (2007) Gene therapy clinical trials worldwide to 2007-an update. *J. Gene Med. 9*, 833−842.
(5) Verma, I. M., and Somina, N. (1997) Gene therapy-promises, problems and prospects. *Nature 389*, 239−242.
(6) Zhang, S., Zhao, Y., Zhao, B., and Wang, B. (2010) Hybrids of nonviral vectors for gene delivery. *Bioconjugate Chem. 21*, 1003−1009.
(7) Anderson, W. F. (1998) Human gene therapy. *Nature 392*, 25−30.
(8) Seow, W. Y., and Yang, Y. Y. (2009) A class of cationic triblock amphiphilic oligopeptides as efficient gene-delivery vectors. *Adv. Mater. 21*, 86−90.
(9) Sun, Y. X., Zeng, X., Meng, Q. F., Zhang, X. Z., Cheng, S. X., and Zhuo, R. X. (2008) The influence of RGD addition on the gene transfer characteristics of disulfide-containing polyethyleneimine/DNA complexes. *Biomaterials 29*, 4356−4365.
(10) Akhtar, S. (2006) Non-viral cancer gene therapy: beyond delivery. *Gene Ther. 13*, 739−740.
(11) Lo, S. L., and Wang, S. (2008) An endosomolytic Tat peptide produced by incorporation of histidine and cysteine residues as a nonviral vector for DNA transfection. *Biomaterials 29*, 2408−2414.
(12) Renigunta, A., Krasteva, G., König, P., Rose, F., Klepetko, W., Grimminger, F., Seeger, W., and Hanze, J. (2006) DNA transfer into human lung cells is improved with Tat-RGD peptide by caveoli-mediated endocytosis. *Bioconjugate Chem. 17*, 327−334.
(13) Wang, C. H., Qiao, L., Zhang, Q., Yan, H. S., and Liu, K. (2012) Enhanced cell uptake of superparamagnetic iron oxide nanoparticles throughdirect chemisorption of FITC-Tat-PEG_{600}-*b*-poly(glycerol monoacrylate). *Int. J. Pharmaceut. 430*, 372−380.
(14) Vivès, E., Brodin, P., and Lebleu, B. (1997) Truncated HIV-1 tat protein basic domain rapidly translocates through the plasma membrane and accumulates in the cell nucleus. *J. Biol. Chem. 272*, 16010−16017.
(15) Guo, Q. G., Zhao, G. J., Hao, F. J., and Guan, Y. F. (2012) Effects of the TAT peptide orientation and relative location on the protein transduction efficiency. *Chem. Biol. Drug Des. 79*, 683−690.
(16) Ko, Y. T., Hartner, W. C., Kale, A., and Torchilin, V. P. (2009) Gene delivery into ischemic myocardium by double-targeted lipoplexes with anti-myosin antibody and TAT peptide. *Gene Ther. 16*, 52−59.
(17) Alhaj Saleh, A. F., Aojula, H. S., and Pluen, A. (2007) Enhancement of gene transfer using YIGSR Analog of Tat-derived peptide. *Biopolymers 89*, 62−71.
(18) Rajagopalan, R., Xavier, J., Rangaraj, N., Rao, N. M., and Gopal, V. (2007) Recombinant fusion proteins TAT-Mu, Mu and Mu-Mu mediate efficient non-viral gene delivery. *J. Gene Med. 9*, 275−286.
(19) Capecchi, M. R. (1980) High efficiency transformation by direct microinjection of DNA into cultured mammalian cells. *Cell 22*, 479−488.

(20) Pouton, C. W., Wagstaff, K. M., Roth, D. M., Moseley, G. W., and Jans, D. A. (2007) Targeted delivery to the nucleus. *Adv. Drug Delivery Rev. 59*, 698−717.
(21) Trabulo, S., Mano, M., Faneca, H., Cardoso, A. L., Duarte, S., Henriques, A., Paiva, A., Gomes, P., Simoes, S., and de Lima, M. C. P. (2008) S4(13)-PV cell penetrating peptide and cationic liposomes act synergistically to mediate intracellular delivery of plasmid DNA. *J. Gene Med. 10*, 1210−1222.
(22) Bremner, K. H., Seymour, L. W., Logan, A., and Read, M. L. (2004) Factors influencing the ability of nuclear localization sequence peptides to enhance nonviral gene delivery. *Bioconjugate Chem. 15*, 152−161.
(23) Schainfeld, R. M., and Isner, J. M. (1999) Critical limb ischemia: nothing to give at the office? *Ann. Intern. Med. 130*, 442−444.
(24) Park, B., Hoffman, A., Yang, Y. G., Yan, J. L., Tie, G. D., Bagshahi, H., Nowicki, P. T., and Messina, L. M. (2010) Endothelial nitric oxide synthase affects both early and late collateral arterial adaptation and blood flow recovery after induction of hind limb ischemia in mice. *J. Vasc. Surg. 51*, 165−173.
(25) Shintani, S., Murohara, T., Ikeda, H., Ueno, T., Sasaki, K., Duan, J. L., and Imaizumi, T. (2001) Augmentation of postnatal neovascularization with autologous bone marrow transplantation. *Circulation 103*, 897−903.
(26) Tateno, K., Minamino, T., Toko, H., Akazawa, H., Shimizu, N., Takeda, S., Kunieda, T., Miyauchi, H., Oyama, T., Matsuura, K., Nishi, J., Kobayashi, Y., Nagai, T., Kuwabara, Y., Iwakura, Y., Nomura, F., Saito, Y., and Komuro, I. (2006) Critical roles of muscle-secreted angiogenic factors in therapeutic neovascularization. *Circ. Res. 98*, 1194−1202.
(27) Kalka, C., Masuda, H., Takahashi, T., Kalka-Moll, W. M., Silver, M., Kearney, M., Li, T., Isner, J. M., and Asahara, T. (2000) Transplantation of ex vivo expanded endothelial progenitor cells for therapeutic neovascularization. *Proc. Natl. Acad. Sci. U.S.A. 97*, 3422−3427.
(28) Koiwaya, H., Sasaki, K. I., Ueno, T., Yokoyama, S., Toyama, Y., Ohtsuka, M., Nakayoshi, T., Mitsutake, Y., and Imaizumi, T. (2011) Augmented neovascularization with magnetized endothelial progenitor cells in rats with hind-limb ischemia. *J. Mol. Cell Cardiol. 51*, 33−40.
(29) Carmeliet, P. (2003) Angiogenesis in health and disease. *Nat. Med. 9*, 653−660.
(30) Wolff, T., Mujagic, E., Gianni-Barrera, R., Fueglistaler, P., Helmrich, U., Misteli, H., Gurke, L., Heberer, M., and Banfi, A. (2012) FACS-purified myoblasts producing controlled VEGF levels induce safe and stable angiogenesis in chronic hind limb ischemia. *J. Cell Mol. Med. 16*, 107−117.
(31) Chen, J. X., Wang, H. Y., Quan, C. Y., Xu, X. D., Zhang, X. Z., and Zhuo, R. X. (2010) Amphiphilic cationic lipopeptides with RGD sequences as gene vectors. *Org. Biomol. Chem. 8*, 3142−3148.
(32) Krichevsky, A., Rusnati, M., Bugatti, A., Waigmann, E., Shohat, S., and Loyter, A. (2005) The fd phage and a peptide derived from its p8 coat protein interact with the HIV-1 Tat-NLS and inhibit its biological functions. *Antivir. Res. 66*, 67−78.
(33) Zeng, X., Sun, Y. X., Qu, W., Zhang, X. Z., and Zhuo, R. X. (2010) Biotinylated transferrin/avidin/biotinylated disulfide containing PEI bioconjugates mediated p53 gene delivery system for tumor targeted transfection. *Biomaterials 31*, 4771−4780.
(34) Yi, W. J., Yang, J., Li, C., Wang, H. Y., Liu, C. W., Tao, L., Cheng, S. X., Zhuo, R. X., and Zhang, X. Z. (2012) Enhanced nuclear import and transfection efficiency of TAT peptide-based gene delivery systems modified by additional nuclear localization signals. *Bioconjugate Chem. 23*, 125−134.
(35) Chung, T. H., Wu, S. H., Yao, M., Lu, C. W., Lin, Y. S., Hung, Y., Mou, C. Y., Chen, Y. C., and Huang, D. M. (2007) The effect of surface charge on the uptake and biological function of mesoporous silica nano-particles in 3T3-L1 cells and human mesenchymal stem cells. *Biomaterials 28*, 2959−2966.
(36) Lee, P. W., Hsu, S. H., Tsai, J. S., Chen, F. R., Huang, P. J., Ke, C. J., Liao, Z. X., Hsiao, C. W., Lin, H. J., and Sung, H. W. (2010) Multifunctional core-shell polymeric nanoparticles for transdermal DNA delivery and epidermal Langerhans cells tracking. *Biomaterials 31*, 2425−2434.
(37) Sun, G., Shen, Y. I., Kusuma, S., Fox-Talbot, K., Steenbergen, C. J., and Gerecht, S. (2011) Functional neovascularization of biodegradable dextran hydrogels with multiple angiogenic growth factors. *Biomaterials 32*, 95−106.
(38) Richardson, T. P., Peters, M. C., Ennett, A. B., and Mooney, D. J. (2001) Polymeric system for dual growth factor delivery. *Nat. Biotechnol. 19*, 1029−1034.
(39) Holash, J., Maisonpierre, P. C., Compton, D., Boland, P., Alexander, C. R., Zagzag, D., Yancopoulos, G. D., and Wiegand, S. J. (1999) Vessel cooption, regression, and growth in tumors mediated by angiopoietins and VEGF. *Science 284*, 1994−1998.
(40) Coultas, L., Chawengsaksophak, K., and Rossant, J. (2005) Endothelial cells and VEGF in vascular development. *Nature 438*, 937−945.
(41) Moritani, S., Kushima, R., Sugihara, H., Bamba, M., Kobayashi, T. K., and Hattori, T. (2002) Availability of CD10 immunohistochemistry as a marker of breast myoepithelial cells on paraffin sections. *Modern Pathol. 15*, 397−405.
(42) Zocchi, M. R., Ferrero, E., Leone, B. E., Rovere, P., Bianchi, E., Toninelli, E., and Pardi, R. (1996) CD31/PECAM-1-driven chemokine-independent transmigration of human T lymphocytes. *Eur. J. Immunol. 26*, 759−767.
(43) Thorin, E., and Shreeve, S. M. (1998) Heterogeneity of vascular endothelial cells in normal and disease states. *Pharmacol. Ther. 78*, 155−166.
(44) Wang, D., Stockard, C. R., Harkins, L., Lott, P., Salih, C., Yuan, K., Buchsbaum, D., Hashim, A., Zayzafoon, M., Hardy, R., Hameed, O., Grizzle, W., and Siegal, G. P. (2008) Immunohistochemistry for the evaluation of angiogenesis in tumor xenografts. *Biotech. Histochem. 83*, 179−189.
(45) Ushijima, C., Tsukamoto, S., Yamazaki, K., Yoshino, I., Sugio, K., and Sugimachi, K. (2001) High vascularity in the peripheral region of non-small cell lung cancer tissue is associated with tumor progression. *Lung Cancer 34*, 233−241.
(46) Norrby, K., and Ridell, B. (2003) Tumour-type-specific capillary endothelial cell stainability in malignant B-cell lymphomas using antibodies against CD31, CD34 and Factor VIII. *Apmis 111*, 483−489.